European Journal of Remote Sensing

ISSN: (Print) 2279-7254 (Online) Journal homepage: https://www.tandfonline.com/loi/tejr20

Above-ground biomass estimation for *Quercus rotundifolia* using vegetation indices derived from high spatial resolution satellite images

Fabrício L. Macedo, Adélia M. O. Sousa, Ana Cristina Gonçalves, José R. Marques da Silva, Paulo A. Mesquita & Ricardo A. F. Rodrigues

To cite this article: Fabrício L. Macedo, Adélia M. O. Sousa, Ana Cristina Gonçalves, José R. Marques da Silva, Paulo A. Mesquita & Ricardo A. F. Rodrigues (2018) Above-ground biomass estimation for *Quercus rotundifolia* using vegetation indices derived from high spatial resolution satellite images, European Journal of Remote Sensing, 51:1, 932-944, DOI: 10.1080/22797254.2018.1521250

To link to this article: https://doi.org/10.1080/22797254.2018.1521250

Published online: 03 Oct 2018.

EUROPEAN JOURNAL OF REMOTE SENSING
2018, VOL. 51, NO. 1, 932–944
https://doi.org/10.1080/22797254.2018.1521250

Taylor & Francis
Taylor & Francis Group

Above-ground biomass estimation for *Quercus rotundifolia* using vegetation indices derived from high spatial resolution satellite images

Fabrício L. Macedo[a], Adélia M. O. Sousa[b], Ana Cristina Gonçalves[b], José R. Marques da Silva[b], Paulo A. Mesquita[b] and Ricardo A. F. Rodrigues[c]

[a]Centro de Investigação e de Tecnologias Agro-Ambientais e Biológicas (CITAB), Universidade de Trás-os-Montes e Alto Douro, Vila Real, Portugal; [b]Departamento de Engenharia Rural, Escola de Ciências e Tecnologia, Instituto de Ciências Agrárias e Ambientais Mediterrânicas (ICAAM), Instituto de Investigação e Formação Avançada, Universidade de Évora Apartado 94, Évora, Portugal; [c]Departamento de Fitossanidade, Engenharia Rural e Solos, Universidade Estadual Paulista – UNESP/FE Campus de Ilha Solteira, Ilha Solteira, SP, Portugal

ABSTRACT

The estimation of vegetation parameters, such as above-ground biomass, with high accuracy using remote sensing data, represents a promising approach. The present study develops models to estimate and map above-ground biomass of Mediterranean *Quercus rotundifolia* stands using one QuickBird satellite image in pan-sharpened mode, with four multispectral bands (blue, green, red and near infrared) and a spatial resolution of 0.70 m. The satellite image was orthorectified, geometrically and radiometrically corrected. Object-oriented classification methods and multi-resolution segmentation were used to derive a vegetation mask per forest species. Data from forest inventory (24 plots) and vegetation indices (NDVI, EVI, SR and SAVI) derived from high spatial resolution satellite images were used for an area of 133 km^2, in southern Portugal. The statistical analysis included correlation, variance analysis and linear regression. The linear regression models fitted included the arithmetic mean and the median values of the vegetation indices per inventory plot as explanatory variables. The overall results of the fitted models show a trend of better performance for those with the median value of the vegetation index as the explanatory variable. The best fitted model (R^2 = 75.3) was associated with the Simple Ratio (SR) median value as an explanatory variable. A *Quercus rotundifolia* above-ground biomass map was produced.

ARTICLE HISTORY
Received 21 February 2017
Revised 16 August 2018
Accepted 5 September 2018

KEYWORDS
Above-ground biomass; high spatial resolution; vegetation indices; linear regression

Introduction

The CO_2 accumulation in the atmosphere has a great contribution from two activities, burning of fossil fuels and deforestation (Watzlawick, Koehler, & Kirchner, 2006), which led to an increase of studies related to biomass evaluation and carbon sequestration (Melo & Durigan, 2006), such as the sustainable forest management, timber management, forest productivity prediction, carbon sink evaluation and the global carbon cycle (Brown, Schroeder, & Kern, 1999; Houghton, 2005; Lu, 2006; Palacios-Orueta, Chuvieco, Parra, & Carmona-Moreno, 2005; Ryu, Chen, Crow, & Saunders, 2004).

Allometric functions at tree-level species and site-specific are most commonly used to estimate biomass, frequently with diameter at breast height and total height as explanatory variables (Flombaum & Sala, 2007; Foroughbakhch, Reyes, Alvarado-Vázquez, Hernández-Piñero, & Rocha-Estrada, 2005; Nelson et al., 1999; Parresol, 1999; Peichl & Arain, 2006; Segura & Kanninen, 2005).

Improvements in remote sensing technology enhanced the development of functions to estimate biomass and carbon stocks (Watzlawick & Kirchner, 2004), using different sensors with different spatial resolution. According to Navulur (2006), this data is classified depending on the pixel size: coarse (30 m or greater), medium (2.0–30 m), high (0.5–2.0 m) and very high (lower than 0.5 m) spatial resolution. With the purpose of estimating biomass and carbon stocks, several studies have been developed using coarse spatial resolution data (Baccini, Laporte, Goetz, Sun, & Dong, 2008; Dong et al., 2003; Yin et al., 2015) or high and very high spatial resolution (Baccini, Friedl, Woodcock, & Warbington, 2004; Häme, Salli, Andersson, & Lohi, 1997; Lu, 2006; Muukkonen & Heiskanen, 2007; Sousa, Gonçalves, Mesquita, & Marques da Silva, 2015; Viana, Aranha, Lopes, & Cohen, 2012). These indirect methods have a better cost-benefit relation and much less time is needed for the assessment when compared with methods based on forest inventory plots and extrapolation methods. Due to their flexibility, it is also possible to analyse the above-ground biomass variation within different regions or in time, as well as the impact of disturbances, such as deforestation or fire (Potter, 1999).

CONTACT Adélia M. O. Sousa asousa@uevora.pt Departamento de Engenharia Rural, Escola de Ciências e Tecnologia, Instituto de Ciências Agrárias e Ambientais Mediterrânicas (ICAAM), Instituto de Investigação e Formação Avançada, Universidade de Évora, Apartado 94, Évora, Portugal

IKONOS, WorldView-2 and QuickBird images, with high spatial resolution, have been used to study biomass in oil palm plantations in Africa (Thenkabail et al., 2004); tree parameters in Amazon forest (Palace, Keller, Asner, Hagen, & Braswell, 2008); structural parameters in *Pinus* forest in Central Spain (Gómez, Wulder, Montes, & Delgado, 2012); biomass in high-density biomass wetlands vegetation (Mutanga, Adam, & Cho, 2012); forest attributes and above-ground biomass in boreal forest stands in Canada (Mora, Wulder, White, & Hobart, 2013); above-ground biomass in mangrove forests in Thailand (Hirata et al., 2014) and in desert steppe ecosystems in Mongolia (Ren & Zhou, 2014); and forest biomass in Chile and Germany (Maack et al., 2015). Using GeoEye-1 and Pleiades-1A images, Clerici, Rubiano, Abd-Elrahman, Hoestettler, and Escobedo (2016) developed a methodology to estimate above-ground biomass in a complex forest in the Colombian Andes. This satellite data can produce detailed spatial distribution biomass maps that are often impossible to acquire using coarser resolutions due to the mixed pixel effects (Wulder, Hall, & Franklin, 2004). Most of these studies use vegetation indices that are mathematical functions that combine two or more spectral bands, condensing data in a quantitative numeric manner (Rizzi, 2004). This spectral information contributes to the differentiation and identification of tree species, and are related to some important biophysical properties, such as leaf area index, biomass and vegetation cover (Ahmed, Tian, Zhang, & Ting, 2011; Ghiyamat, Shafri, & Shariff, 2016) and have been used to develop above-ground biomass functions (Chen, Weber, & Gokhale, 2011; Hall, Skakun, Arsenault, & Case, 2006; Ji et al., 2012; Lu, 2006; Muukkonen & Heiskanen, 2007; Tomppo, Nilsson, Rosengren, Aalto, & Kennedy, 2002).

According to Ferreira, Ferreira, and Ferreira (2008) and Mutanga et al. (2012) the vegetation indices based on red (RED) and near-infrared (NIR) bands are directly related to the photosynthetic activity of vegetation, such as NDVI for which good results for biomass estimation were attained in tropical landscapes (Foody, Boyd, & Cutler, 2003; Steininger, 2000), as well as in Mediterranean evergreen oaks and shrublands (Calvão & Palmeirim, 2004; Carreiras, Pereira, & Pereira, 2006; Pereira, Oliveira, & Paul, 1995; Viana et al., 2012), biomass, volume and basal area (Maciel, Bastos, Carvalho, & Watrin, 2009) and above-ground biomass and carbon stocks (Clerici et al., 2016).

For the Mediterranean region, Gómez et al. (2012) explored the potential of QuickBird images in pine forest structure characterisation to assess wood volume and biomass, as quadratic mean diameter, basal area and number of trees per unit area, using the Classification and Regression Trees (CART) method; Viana et al. (2012) analysed different approaches to estimating crown biomass of *Pinus pinaster* stands and shrubland above-ground biomass with a remote sensing predictor in order to obtain large-scale forest biomass mapping. However, above-ground biomass estimation for holm oak (*Quercus rotundifolia*) using high spatial resolution remote sensing data and vegetation indices was not found in the literature.

Quercus rotundifolia is one of the most important forest trees in the dry areas of the Iberian Peninsula. This species is native to the Mediterranean basin and distributed from Portugal to Syria (Forey, 1996; Valdés, Talavera, & Fernández-Galiano, 1987). According to the national forest inventory, in Portugal holm oak stands account for approximately 413,000 ha, corresponding to 13.0% of the Portuguese forest area with 27.4% being located in Alentejo (IFN5, 2010). Holm oak usually occurs in low-density stands in a silvopastoral system, called *montado*, with open heterogeneous canopies, where the main product is the fruit, associated with extensive grazing. However, due to the wood's high calorific value, the timber is particularly important for firewood and charcoal, being an alternative source of energy.

The objective of this study is to develop models to estimate above-ground biomass at local and regional scale, using high spatial resolution satellite images, for *Quercus rotundifolia* pure stands for a region of southern Portugal and which could also be used in other regions for the same species, with similar climate and stand characteristics. The main goal was to develop an above-ground biomass empirical model for *Quercus rotundifolia*, dependent on vegetation indices derived from high spatial resolution satellite images (QuickBird, with pixel size of 0.70 m), and map biomass. In literature, the biomass models most frequently use the mean of a vegetation index as an explanatory variable. Nonetheless, if the vegetation index does not have a normal distribution, the arithmetic mean, can result in biased estimations of above-ground biomass. An alternative is to use the median values. In this study both the mean and the median vegetation index values were used to fit the functions and the performance of the models was compared.

Material and methods

Study area

The study area, covering approximately 133 km^2, is located in southern Portugal (central coordinate 8º 4′ 53.98″W and 38º 51′ 16.12″N). This region is characterised by a Mediterranean climate and the terrain is marked by plains, with low altimetry variation (mean elevation of approximately 200 m). The forest is composed mainly of evergreen oaks, namely, holm oak (*Quercus rotundifolia*) and cork oak (*Quercus suber*), with small patches of *Pinus pinaster, Pinus*

pinea and *Eucalyptus globulus* in both pure and mixed stands.

Satellite data

QuickBird satellite data, with 0.70 m of spatial resolution, was used, in pan-sharpened mode, corresponding to the fusion of panchromatic band with four multispectral bands, b1 – blue (0.45–0.52 μm), b2 – green (0.52–0.60 μm), b3 – red (0.63–0.69 μm) and b4 – near infrared (0.76–0.90 μm). The image acquisition date is 7 August 2006, with a mean sun elevation of 65.3º and a mean off Nadir view angle of 12.8º.

The pre-processing methods applied to the image were the geometric and radiometric correction. The geometric correction was done based on ground control points collected with a Global Navigation Satellite System (GNSS) and geodetic vertices identified both on the ground and in the image, using ENVI version 4.8 (ENVI 2009). The Root Mean Square Error (RMSE) was 0.49 m. The image was orthorectified using Rational Polynomial Coefficients (RPCs) based on digital terrain elevation from Advanced Spaceborne Thermal Emission and Reflection Radiometer (ASTER).

The image digital numbers (DN) were converted to Top of Atmosphere (ToA) reflectance. Atmospheric correction was applied using the dark object subtraction method (Chavez, 1988), which allows to obtain top-of-canopy and soil reflectance (Huete, Miura, Yoshioka, Ratana, & Broich, 2014).

A vegetation mask per forest species was obtained based on satellite image, where the trees crowns were delimited and identified by specie. For this purpose, the object-oriented classification image methods were used. The image classification was based on objects instead of pixels, contrary to the traditional image classification (Frohn, Autrey, Lane, & Reif, 2011). Three main steps were followed all executed in the eCognition Developer software v. 8.0.1 (Definiens Imaging, 2010) (Figure 1), (i) contrast split segmentation algorithm, the variables considered were the QuickBird bands and the Normalized Difference Vegetation Index, NDVI (Rouse, Haas, Schell, & Deering, 1973), calculated based on the difference between NIR and RED bands, isolating the tree crowns from the other land use and vegetation types; (ii) multiresolution segmentation method, was used to isolate and delimit the tree crowns or clusters of tree crowns within the resulting objects from the previous step. For this purpose, scale compactness and shape parameters, with thresholds chosen empirically from parameters such as tone or spatial pattern; (iii) the objects representing tree crowns and tree crowns clusters were classified per forest species using the nearest neighbour classification method (for more details on methodology see Sousa, Mesquita, Gonçalves, and Marques da Silva (2010).

The study area was divided into a 45.5 m x 45.5 m (2,070.25 m^2) grid, equivalent to 65 by 65 image pixels with 0.70 m of spatial resolution. The vegetation mask per species was used to determine composition per grid as well as crown cover in percentage, using a GIS software ArcGIS Desktop v.10.4 (Esri, 2010). When crown cover of one species was equal to or larger than 75%, the grid was considered pure. Pure grids of *Quercus rotundifolia* were divided into two strata: (i) 10% to 30% crown cover; and (ii) crown cover higher than 30%. Forest inventory plots, each corresponding to one grid, were selected by random stratified sampling, by proportional allocation.

Forest inventory

The forest inventory data set, collected in 2011, is composed of 24 pure plots, of which 15 are monospecies and 9 are multispecies of *Quercus rotundifolia* and *Quercus suber*. All individuals with a diameter at breast height of 6 cm or greater belong to the main stand. For these trees, dendrometric parameters were measured, namely diameter at breast height, total height and crown radii in 4 directions (North, South, East and West) (Avery & Burkhart, 1994) and their geographical location was recorded by GNSS. Above-ground biomass per tree (Eq. 4) was estimated using the allometric functions equations (1) – (3) of Paulo and Tomé (2006), where *ww, wb* and *wc* are respectively the biomass of wood (in kg); bark (in kg); and crown (in kg); d is the tree diameter at breast height (in cm) and *AGB* is the above-ground biomass (in kg). Above-ground biomass per plot was calculated as the sum of all trees biomass per area unit (t/ha).

$$ww = 0.164185 \times d^{2.011002} \quad (1)$$

$$wb = 0.600169 \times d^{1.355957} \quad (2)$$

$$wc = 1.909152 \times d^{1.200354} \quad (3)$$

$$AGB = ww + wb + wc \quad (4)$$

Vegetation indices

Vegetation absorbs energy selectively. Due to the photosynthetic pigments the leaves absorb predominantly in the RED region of the electromagnetic spectrum, while due to their internal structure they reflect in the NIR. The vegetation indices use the combination of these bands to quantify and maximize the contrast of reflectance in these two spectrum regions and relate it to the plants' properties (Berra

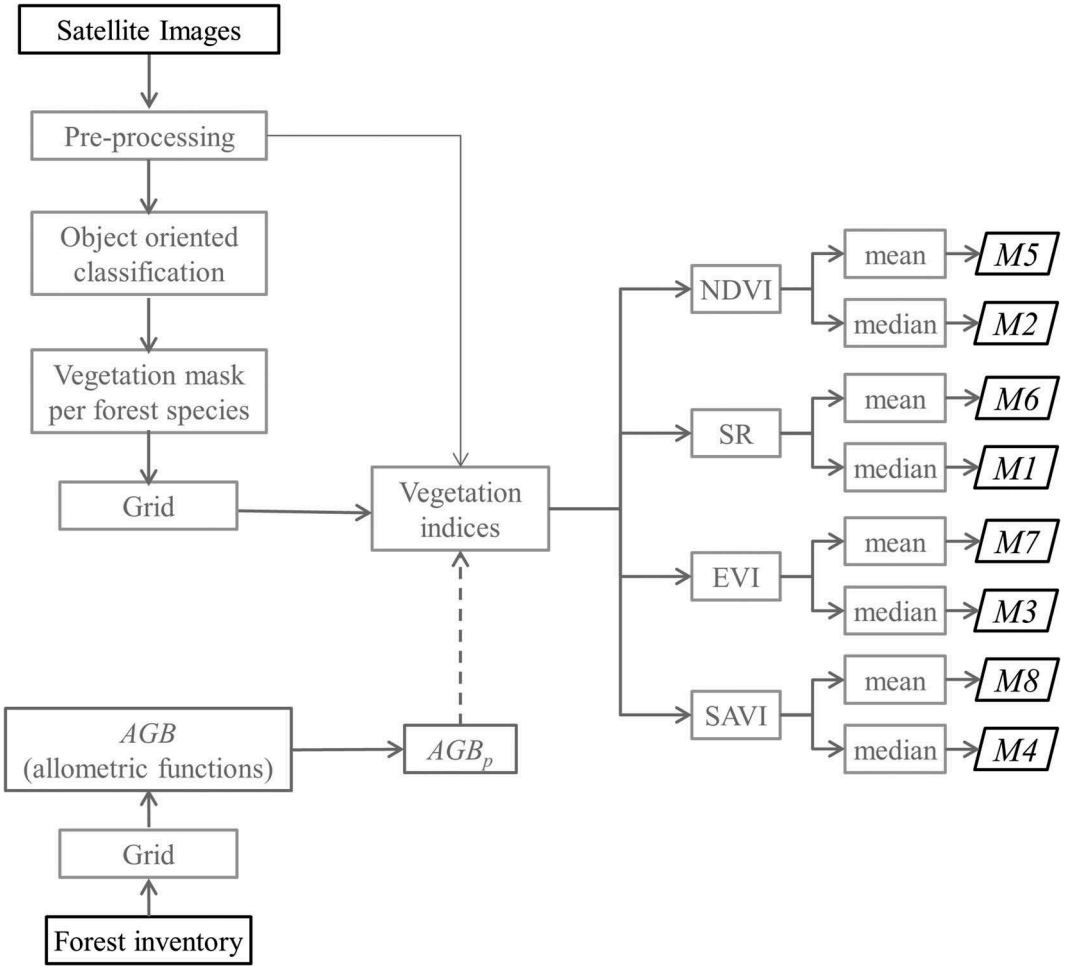

Figure 1. Conceptual scheme of the applied methodology.

et al., 2012; Mutanga & Skidmore, 2004; Ponzoni & Shimabukuro, 2007; Van Der Meer et al., 2016).

Four vegetation indices were calculated based on the individual bands of a QuickBird image, using Spatial Analyst by ArcGIS (Esri, 2010), namely (Table 1): the Normalized Difference Vegetation Index (NDVI); the Enhanced Vegetation Index (EVI); the Simple Ratio (SR); and the Soil-Adjusted Vegetation Index (SAVI). All combine information from two or more spectral bands to enhance vegetation signal while minimising soil, atmospheric and solar irradiance effects (Jackson & Huete, 1991).

NDVI is the most extensively used vegetation index, based on the fact that vegetation is highly reflective in the NIR region and strongly absorbing in the RED (Rouse et al., 1973). EVI was developed to optimize the vegetation signal with improved sensitivity in high biomass areas and improved vegetation monitoring by reducing the impact of canopy background noise and atmospheric influences (Huete, Justice, & Van Leuwen, 1996; Huete, Liu, Batchily, & Leeuwen, 1997). SR is calculated by dividing the NIR and RED band (Jordan, 1969) and intends capture the contrast between the RED and NIR bands for vegetated pixels. SAVI was developed by Huete (1988) especially for areas with sparse vegetation cover, to reduce the soil background confounding effects. The L values vary from 0 to 1, for areas of 100% and 0% crown cover or no vegetation, respectively. According to the same author, L = 0.5 is reasonable for a wide range of soil types. In this study the crown cover presents some variation, so the primarily recommended L-value was used (L = 0.5).

Table 1. QuickBird-derived vegetation indices used to estimate above-ground biomass.

Vegetation Index	Equation	Reference
Normalized Difference Vegetation Index	$NDVI = \frac{NIR - RED}{NIR + RED}$	(Rouse et al., 1973)
Enhanced Vegetation Index	$EVI = \frac{2.5 \times (NIR - RED)}{(NIR + 6 \times RED - 7.5 \times BLUE + 1)}$	(Huete et al., 1996; Huete et al., 1997)
Simple Ratio	$SR = \frac{NIR}{RED}$	(Jordan, 1969)
Soil Adjusted Vegetation Index	$SAVI = \frac{(NIR - RED)}{(NIR + RED + L)} \times (L + 1)$	(Huete, 1988)

Statistical analysis and above-ground biomass estimation

Statistical analysis included correlation analysis, variance analysis and linear regression. The first was carried out with the Spearman correlation test, as data had a non-normal distribution assessed with the Shapiro Wilk normality test (Shapiro, Wilk, & Chen, 1968). The variance analysis between the mean and median values of the vegetation indices was done with a non-parametric test, the Wilcoxon test, as variables did not meet normality assumptions (Sheskin, 2007). For the latter the ordinary least squares linear regression (Eq. 5, where β_O is the constant, β_1 the slope and VI the vegetation index) was used, as suggested by several authors (eg Austin, Mackey, & Van Niel, 2003; Drake et al., 2002a; Drake, Dubayah, Knox, Clark, & Blair, 2002b; Popescu, Wynne, & Nelson, 2003; Rauste & HäMe, 1994). The vegetation index value per grid was calculated as the arithmetic mean and the median of all pixels within each grid. The statistical properties of the models allow the selection of functions that potentially fit the data better and/or present better predictive ability (Burkhart & Tomé, 2012; Pretzsch, 2009). These were evaluated using the sum of squares of the residuals (SQR), the coefficient of determination (R^2) and the adjusted coefficient of determination (R^2_{aj}). Complementary PRESS (Eq. 6, where y are the observed values, $\hat{y}$ are the estimated values, i is the number of the observation, i = 1…n) and APRESS (Eq. 7) and their average values (PRESSm and APRESSm) statistics were used. The first is the sum of the square of the PRESS residuals and the second the sum of the absolute value of PRESS residuals. According to Clutter, Fortson, Pienaar, Briester, and Bailey (1983) and Myers (1986) these criteria can be used as a true validation test, considering the best model to be the one that has the lowest PRESS and APRESS values. The models were ranked according to the aforementioned criteria and the best model was the one with the lowest values. The heteroscedasticity associated with the error term of the models was evaluated graphically, plotting the studentised residuals against the estimated values. The normality of the studentised residuals was carried out using the normal Quantile – Quantile plots (QQ plots) and with the Shapiro Wilk normality test, for a probability level of 0.001 (Montgomery & Peck, 1982; Myers, 1986). The statistical analysis was implemented in R statistical software (R Development Core Team, 2012).

$$AGB = \beta_O + \beta_1 \times VI \tag{5}$$

$$\mathrm{PRESS} = \sum_{i=1}^{n} \left(y_i - \hat{y}_{i,-1}\right)^2 \tag{6}$$

$$\mathrm{APRESS} = \sum_{i=1}^{n} \left|y_i - \hat{y}_{i,-1}\right| \tag{7}$$

The main steps of the methodology applied in this study are presented in the workflow diagram presented in Figure 1.

Results and discussion

Figure 2 shows the result of the multi-resolution segmentation and object-oriented classification process for a small area of the image, used for *Quercus rotundifolia* pure stands. The agreement between the classification and ground truth obtained by the Kappa statistic (Congalton, Oderwald, & Mead, 1983; Stehman, 1996) was 78% and the global precision was 89%. The kappa statistic level of agreement is indicative that the methodology used to obtain the vegetation mask, for tree crown delimitation, has a good performance. Two reasons can be identified for the results attained. The first is the contrast, or the different spectral response, between the tree crowns and other land uses, especially those of the understory vegetation. The acquisition date of the images was August, which in the Mediterranean region corresponds to a warm and dry season and the end of the phenological cycle of the vegetation of the understorey. Thus, while the tree crowns of *Quercus rotundifolia* are photosynthetically active, the other vegetation has no photosynthetic activity, which enhances the contrast of the reflective response of the trees and the understorey vegetation, resulting in good tree crown delimitation accuracy. The second reason is related to the tree species identification. Vaz et al. (2011) analysed these two forest species, concluding that *Quercus suber* has higher photosynthetic potential than *Quercus rotundifolia*, which results in higher values of reflectance for *Quercus suber* than for *Quercus rotundifolia*. The spectral response is sufficiently different between these two species allowing their differentiation with accuracy.

Two other aspects that give some insight into these results are the density and the spatial arrangement of the trees. Most *Quercus rotundifolia* stands are open that is have low number of trees per area unit and as a consequence many trees are isolated, consequently the crowns do not touch each other, and frequently are at a considerable distance from their neighbouring trees, which enables a better delimitation of the tree crowns and species identification. However, and in spite of many trees being isolated, the spatial arrangement is irregular, which means that some trees have a cluster spatial arrangement, although less frequently. In these clusters the separation of the individual tree crowns and species identification is more difficult and sometimes not possible. Nevertheless, as the

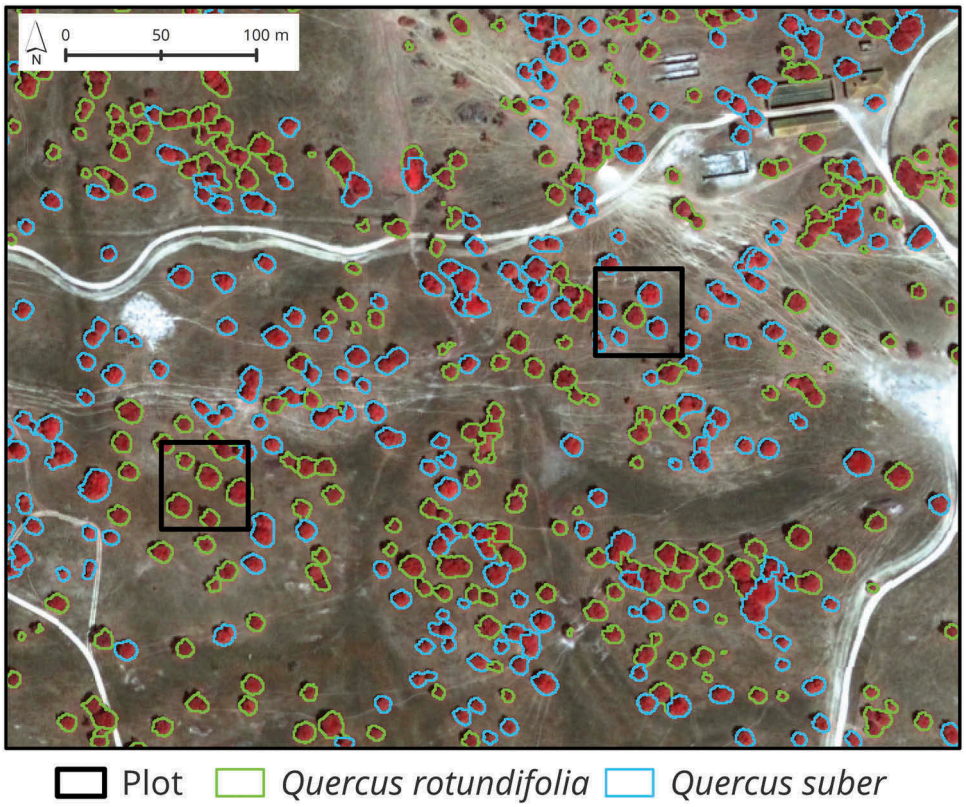

Figure 2. Illustration of the multi-resolution segmentation and object-oriented classification process over the QuickBird image with false colour composite (RGB – NIR, Red, Blue).

number of clusters per area unit is rather small it is possible to obtain a good performance with the methodology used.

Table 2 shows the descriptive statistics for the data considered in this study. The multispecies plots have a number of *Quercus suber* individuals of 5 treesha^{-1} in 6 plots, 10 treesha^{-1} in one and 14 treesha^{-1} in two, corresponding to an average of about 15% of the stems. The stem diameters vary between 8.7 cm and 84.7 cm and the crown diameters between 2.0 m and 13.3 m. Crown cover (CC) varies between 13.7% and 67.6%, covering the two previously defined strata.

Table 2. Above-ground biomass (AGB), Crown cover (CC), Number of trees per hectare (N), Basal area (G) and vegetation indices descriptive statistics (where min is the minimum value, max the maximum value, med the arithmetic mean, SD the standard deviation and CV(%) the coefficient of variation).

	Min	Max	Med	SD	CV (%)
AGB (t/ha)	15.4	45.9	25.9	7.8	29.9
CC (%)	13.7	67.6	33.0	15.0	45.5
N	29.0	140	66.0	27.9	42.4
G (m^2/ha)	3.5	10.6	6.0	1.8	29.2
Mean/plot					
NDVI	0.237	0.339	0.281	0.030	10.6
SR	1.648	2.058	1.817	0.125	6.9
EVI	0.173	0.275	0.215	0.028	12.9
SAVI	0.131	0.205	0.162	0.020	12.5
Median/plot					
NDVI	0.199	0.344	0.261	0.041	15.9
SR	1.497	2.050	1.715	0.158	9.2
EVI	0.157	0.270	0.196	0.034	17.1
SAVI	0.120	0.204	0.150	0.024	16.2

The vegetation indices are relatively different from each other, with SR and EVI having the smallest and the greatest coefficient of variation (CV), respectively. The coefficient of variation for the median values per plot and per vegetation index is larger when compared with the mean values (Table 2).

The Spearman correlation analysis, for a significance level of 95%, showed strong positive correlations between above-ground biomass (AGB) and vegetation indices for their mean and median values per plot, being larger for NDVI and SR (Table 3), corresponding to the vegetation indices with the lower coefficient of variation (Table 2).

In accordance with our results, positive correlations were found by Pinheiro, Durigan, and Adami (2009) for NDVI (0.481), SR (0.443) and SAVI (0.477), though weaker. The difference can be explained by the different development of shrub layers in both stands; in our study the shrub layer had low density while in that of Pinheiro et al. (2009) it had high density.

Contrary to our results, in the work of Watzlawick, Kirchner, and Sanquetta (2009) on *Araucaria angustifolia* stands and of Watzlawick et al. (2006) on *Pinus taeda* stands, both with very high density, found negative correlations between biomass and NDVI (–0.740 and –0.800, respectively) and SR (–0.710 and –0.750, respectively). According to several authors (Ponzoni & Shimabukuro, 2007; Wang,

Table 3. Spearman correlation coefficients for mean and median values per plot.

	Mean						Median					
	AGB (t/ha)	CC (%)	NDVI	EVI	SR	SAVI	AGB (t/ha)	CC (%)	NDVI	EVI	SR	SAVI
AGB (t/ha)	1						1					
CC (%)	0.83	1					0.83	1				
NDVI	0.85	0.95	1				0.80	0.86	1			
EVI	0.75	0.91	0.87	1			0.75	0.87	0.91	1		
SR	0.86	0.96	0.99	0.88	1		0.80	0.86	1.00	0.91	1	
SAVI	0.70	0.84	0.79	0.98	0.81	1	0.70	0.82	0.83	0.97	0.83	1

Adiku, Tenhunen, & Granier, 2005; Zanzarini, Pissara, Brandão, & Teixeira, 2013), an increase in crown cover does not increase NDVI due to its quick saturation, because the index stabilizes, even though the density of the canopy increases, turning it insensible to biomass increase (Jensen, 2000).

The strong correlation coefficients between vegetation indices and above-ground biomass seem to be associated with the time of the year that the image is taken. For Mediterranean countries, in summer (dry season), the understorey has a very light colour, due to the presence of dry vegetation and soil, which maximizes the contrast between the *Quercus rotundifolia* trees and the dry herbaceous background. The image was acquired in august, when the understorey had mainly dry vegetation and soil, resulting in high contrast and also very high correlation coefficients. Accordingly, better results for above-ground biomass estimation using Landsat ETM+ images were obtained in the dry season as opposed to other seasons of the year by Nguyen et al. (2015). The same authors stress that the satellite image data, which is related to the vegetation phenological cycle and season of the year, is a relevant factor in these types of studies, as evaluating the vegetation properties using remote sensing data with a good level of accuracy depends on the contrast in the spectral signatures of the different types of vegetation. Thenkabail et al. (2004) and Carreiras et al. (2006) also refer to this type of phenomena in their studies, for very high and medium spatial resolution images and aerial photos, respectively.

The Wilcoxon test, for a significance level of 95%, showed significant differences between the mean and median values per plot for NDVI ($V = 293$, $p < 0.001$), EVI ($V = 300$, $p < 0.001$), SAVI ($V = 300$, $p < 0.001$) and SR ($V = 300$, $p < 0.001$).

The statistical properties of the models can be seen in Table 4. The results of this study demonstrate that the above-ground biomass models with a vegetation index as an explanatory variable have a good performance, thus confirming that sensitivity can be maximised in the evaluation of the photosynthetically active vegetation (Günlü, Ercanli, Sönmez, & Baskent, 2014). This is related to the accuracy of the delimitation of the tree crowns and species identification, which are dependent on the type of the stand and the contrast of the spectral signature reflectance of the different land uses present, as previously mentioned. The overall analysis of the fitted models reveals that those with the median values of the vegetation indices as an explanatory variable have a better performance than the corresponding models with the mean as an independent variable. This might be related to the non-normality of the values of the vegetation indices. The median, being the midpoint of a frequency distribution of observed values, is not skewed by very large or very small values, thus it is a robust statistic when data does not have normal distribution.

The model with the best performance has the median of SR ($\widetilde{SR}$) as explanatory variable, the simpler vegetation index. When analysing PRESS and APRESS statistics it can be seen that M1 has the lowest values. The best function with mean values per plot is M5, with $\overline{NDVI}$ as independent variable. The models with EVI and SAVI as independent variables have worse statistical properties than those with SR and NDVI, for both the mean and median values per grid. This fact indicates the good relationship between the simplest vegetation indices and certain vegetation parameters, in this case with the above-ground biomass. Analysis of the studentised residuals of M1 and M6 (Figure 3) and M2 and M5 (Figure 4) does not show systematic variations, the graphics of normal probability approach a straight line and the normality of the residuals is not met by the Shapiro-Wilk test.

Table 4. Fitted models statistical properties (AGB in t/ha).

Model	Equation	SQR	R^2	R^2_{aj}	PRESS	APRESS	PRESSm	APRESSm
M1	$AGB = -47.108 + 42.582 \times \widetilde{SR}$	341	**0.753**	**0.742**	0.03631	0.80914	0.00151	0.03371
M2	$AGB = -16.324 + 161.835 \times \widetilde{NDVI}$	347	0.749	0.738	0.03776	0.83321	0.00157	0.03472
M3	$AGB = -11.640 + 191.920 \times \widetilde{EVI}$	430	0.689	0.675	0.04172	0.82026	0.00174	0.03418
M4	$AGB = -10.959 + 245.435 \times \widetilde{SAVI}$	567	0.590	0.571	0.04701	0.81812	0.00196	0.03409
M5	$AGB = -37.026 + 223.808 \times \overline{NDVI}$	354	**0.744**	**0.732**	0.03776	0.83321	0.00157	0.03472
M6	$AGB = -70.757 + 53.207 \times \overline{SR}$	367	0.735	0.723	0.03631	0.80914	0.00151	0.03371
M7	$AGB = -22.156 + 223.995 \times \overline{EVI}$	494	0.643	0.626	0.04172	0.82026	0.00174	0.03418
M8	$AGB = -19.736 + 281.492 \times \overline{SAVI}$	628	0.546	0.525	0.04701	0.81812	0.00196	0.03409

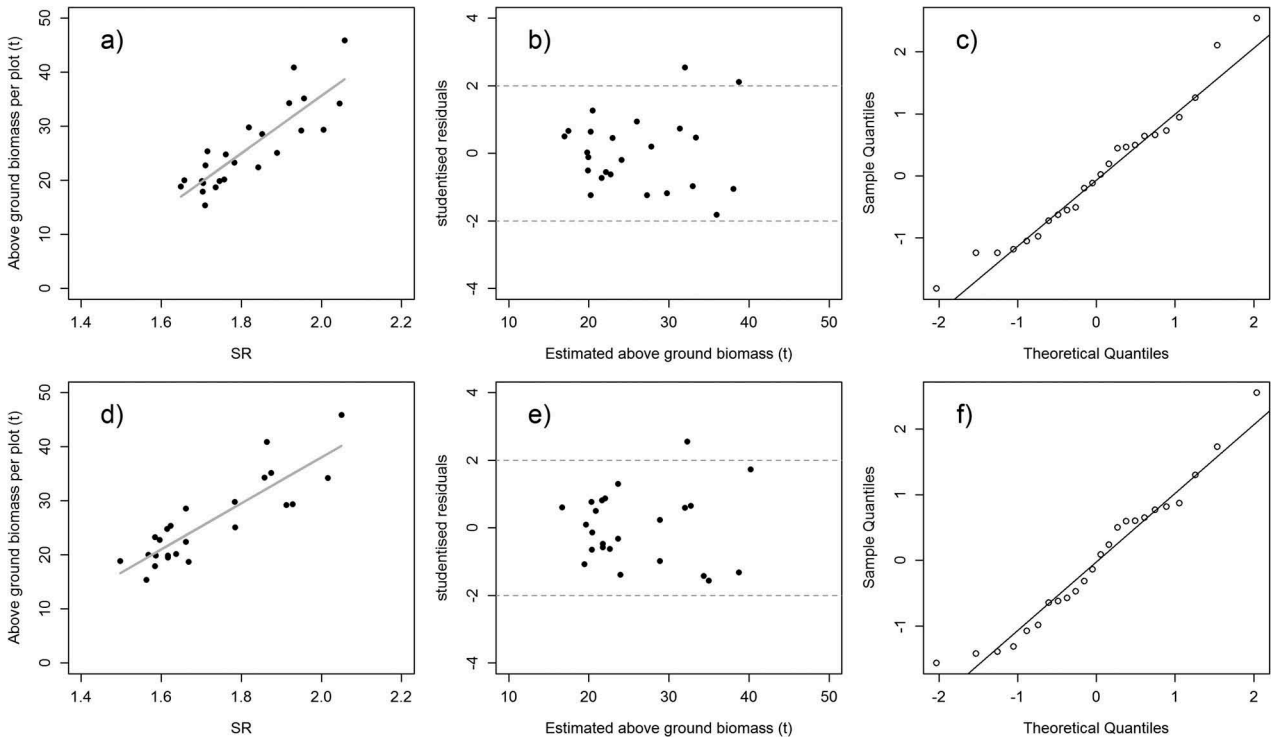

Figure 3. Linear function (a), studentised residuals (b) and graphics of normal probability (c) for M6 and linear function (d), studentised residuals (e) and graphics of normal probability (f) for M1.

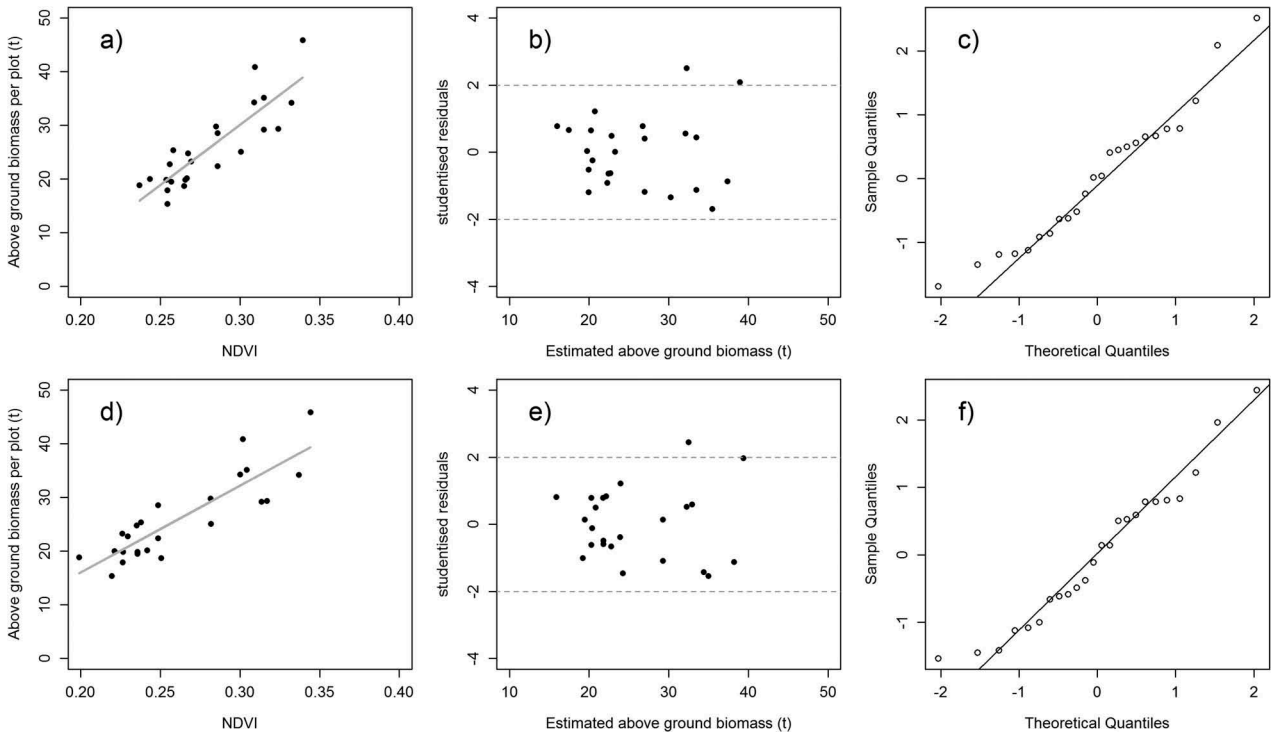

Figure 4. Linear function (a), studentised residuals (b) and graphics of normal probability (c) for M5 and linear function (d), studentised residuals (e) and graphics of normal probability (f) for M2.

In literature few references were found for biomass estimation as a function of vegetation indices using high spatial resolution satellite images. The results of this study are consistent with those of several authors, though with higher coefficients of determination. Thenkabail et al. (2004) reported that the best model for biomass estimation in an oil palm plantation in Africa was a NDVI function with R^2 of 72 %. Clerici et al. (2016) stated that the best model for above-ground biomass estimation for periurban Andean secondary forest was a linear function with the mean value of SR as an independent variable,

with R^2 of 48%. Similarly, other authors (Watzlawick et al., 2009, 2006) reported that simple linear models with SAVI and NDVI as independent variables have the best predictive abilities for above-ground biomass estimates, with an adjusted coefficient of determination of 57% and 53%, respectively. Furthermore, analogous results were found in several studies based on vegetation indices derived from medium and coarse spatial resolution satellite images (Araújo, 1999; Dong et al., 2003; Häme et al., 1997; Maciel et al., 2009).

An example of the application of model M1 for above-ground biomass mapping is presented in Figure 5 for a small area. It was obtained calculating above-ground biomass per grid. It has the advantage of enabling above-ground biomass spatial distribution analysis for the whole study area.

This methodology, which uses high spatial resolution satellite images, makes an important contribution towards forest planning, management and silviculture in decision-making as it allows the production of biomass maps (model applied over a grid) through simple procedures, and is less time-consuming than other methodologies, for example forest inventory and spatial analysis. It is also important to forest inventory design as a more cost-efficient sampling can be achieved at local and regional scale (McRoberts, Tomppo, & Naesset, 2010).

Conclusions

The rapid advancement of remote sensing technology expands the choice of the imagery sources. The increase in the availability of high spatial resolution images allows vegetation studies with a high level of accuracy at different scales.

This study implemented a comprehensive methodological framework for above-ground biomass prediction using high spatial resolution images. The results show that images taken in summer in Mediterranean countries can be used to estimate *Quercus rotundifolia* stands as a function of vegetation indices. The acquisition image date can be a limitation, because for the Mediterranean region high spatial resolution images are not available with high frequency, but similar data may be available from different satellites.

The model with the best predictive ability for estimating above-ground biomass (M1) has the median of SR as an explanatory variable. When comparing the models, those with the median of the vegetation indices showed better accuracy than those with the mean as an independent variable. These results can be explained, at least in part, by the non-normal distribution of the vegetation indices values.

The approach developed can be used in *Quercus rotundifolia* stands with similar stand structure to estimate above-ground biomass. Nonetheless, the swath of these images has a width of 16.5 km at nadir, which is

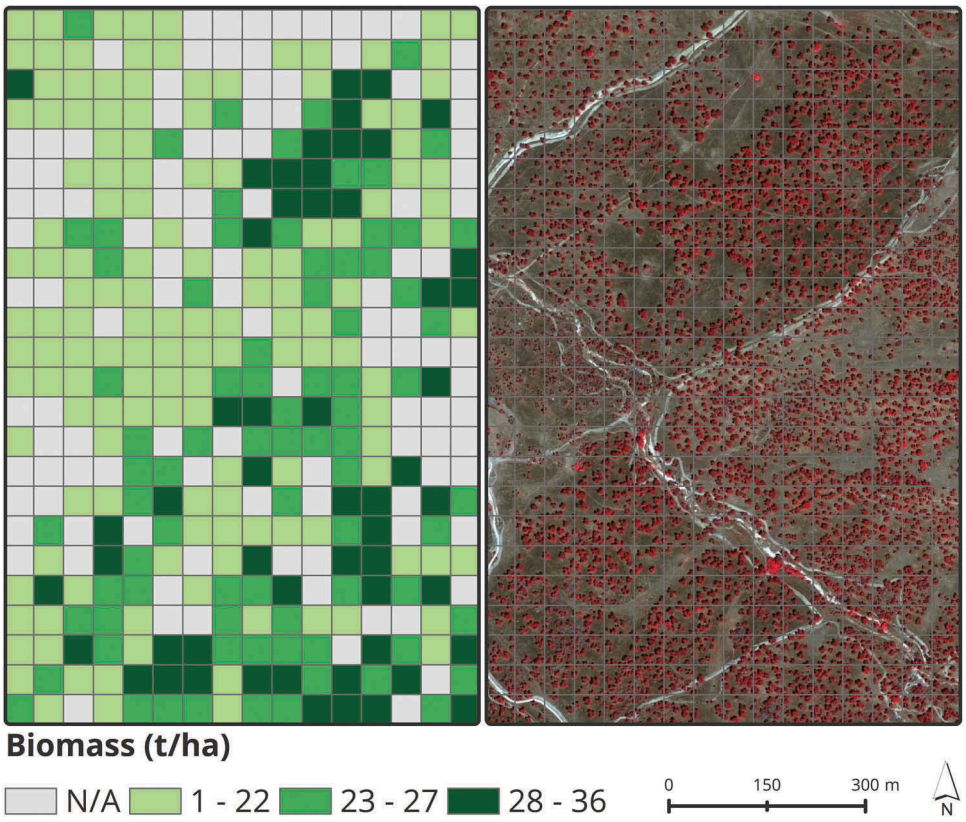

Figure 5. Illustration of model M1 application (left) and a false colour composite image (RGB – NIR, Red, Green) with the grid (right). The grey colour correspond to the grids where the model is not applied (N/A) because they are not pure of holm oak.

adjusted to the local scale. To evaluate large areas several images have to be considered and worked through.

Acknowledgments

The authors are thankful to the: (a) Program of scholarship Ciências sem Fronteiras that allowed the development of this study at Évora University, Portugal; (b) Programa Operativo de Cooperação Transfronteiriço Espanha – Portugal (POCTEP), which funded the project Altercexa – Medidas de Adaptación y Mitigación del Cambio Climático a Través del Impulso de las Energías Alternativas en Centro, Alentejo y Extremadura, within which this study was developed. (Ref[a] 0317_Altercexa_I_4_E and 0406_ALTERCEXA_II_4_E); (c) FEDER Funds through the Operational Program for Competitiveness Factors - COMPETE and National Funds through FCT – Foundation for Science and Technology, under the Strategic Project UID/AGR/00115/2013, which funded this study; (d) TrustEE - innovative market based Trust for Energy Efficiency investments in industry (Project ID: H2020 - 696140); (e) to the forest producers for allowing plot installation and measuring and to the field team, Carla Coelho, David Gomes and Pedro Antunes, for their work in data colleting.

Disclosure statement

No potential conflict of interest was reported by the authors.

Funding

The authors are thankful to the: (a) Program of scholarship Ciências sem Fronteiras that allowed the development of this study at Évora University, Portugal; (b) Programa Operativo de Cooperação Transfronteiriço Espanha - Portugal (POCTEP), which funded the project Altercexa - Medidas de Adaptación y Mitigación del Cambio Climático a Través del Impulso de las Energías Alternativas en Centro, Alentejo y Extremadura, within which this study was developed. (Ref[a] 0317_Altercexa_I_4_E and 0406_ALTERCEXA_II_4_E); (c) FEDER Funds through the Operational Program for Competitiveness Factors - COMPETE and National Funds through FCT – Foundation for Science and Technology, under the Strategic Project UID/AGR/00115/2013, which funded this study; (d) TrustEE – innovative market based Trust for Energy Efficiency investments in industry (Project ID: H2020 - 696140). It has received funding from the European Union's Horizon 2020 research and innovation programme under grant agreement No 696140. The work reflects only the author's view and the Agency and the Commission are not responsible for any use that may be made of the information it contains.

References

Ahmed, T., Tian, L., Zhang, K.C., & Ting, K.C. (2011). A review of remote sensing methods for biomass feedstock production. *Biomass and Bioenergy*, *35*, 2455–2469.

Araújo, L.S. 1999. Análise da cobertura vegetal e de biomassa em áreas de contato floresta/savana a partir de dados TM/LANDSAT e JERS-1. Dissertação (Mestrado em Sensoriamento Remoto), Instituto Nacional de Pesquisas Espaciais, Brazil. 63 101–124

Austin, J.M., Mackey, B.G., & Van Niel, K.P. (2003). Estimating forest biomass using satellite radar: An exploratory study in a temperate Australian Eucalyptus forest. *Forest Ecology and Management*, *176*, 575–583.

Avery, T.E., & Burkhart, H.E. (1994). *Forest measurements* (Fourth ed.). New York, USA: McGraw-Hill, Inc.

Baccini, A., Friedl, M.A., Woodcock, C.E., & Warbington, R. (2004). Forest biomass estimation over regional scales using multisource data. *Geophysical Research Letters*, *31*, 1–4.

Baccini, A., Laporte, N., Goetz, S.J., Sun, M., & Dong, H. (2008). A first map of tropical Africa's above-ground biomass derived from satellite imagery. *Environmental Research Letters*, *3*(4), 045011.

Berra, E.F., Brandelero, C., Pereira, R.S., Sebem, E., Goergen, L.C.G., Benedetti, A.C.P., & Lippert, D.B. (2012). Estimativa do volume total de madeira em espécies de eucalipto a partir de imagens do satélite Landsat. *Ciência Florestal*, *22*, 853–864.

Brown, S.L., Schroeder, P., & Kern, J.S. (1999). Spatial distribution of biomass in forests of the eastern USA. *Forest Ecology and Management*, *123*, 81–90.

Burkhart, H.E., & Tomé, M. (2012). *Modeling forest trees and stands*. Dordrecht: Springer Science & Business Media.

Calvão, T., & Palmeirim, J.M. (2004). Mapping mediterranean scrub with satellite imagery: Biomass estimation and spectral behaviour. *International Journal of Remote Sensing*, *25*, 3113–3126.

Carreiras, J.M.B., Pereira, J.M.C., & Pereira, J.S. (2006). Estimation of tree canopy cover in evergreen oak woodlands using remote sensing. *Forest Ecology and Management*, *223*, 45–53.

Chavez, P.S., Jr. (1988). An improved dark-object subtraction technique for atmospheric scattering correction of multispectral data. *Remote Sensing of Environment*, *24* (3), 459–479.

Chen, F., Weber, K.T., & Gokhale, B. (2011). Herbaceous biomass estimation from SPOT 5 imagery in semiarid rangelands of Idaho. *GIScience & Remote Sensing*, *48*, 195–209.

Clerici, N., Rubiano, K., Abd-Elrahman, A., Hoestettler, J. M.P., & Escobedo, F.J. (2016). Estimating aboveground biomass and carbon stocks in Periurban Andean secondary forests using very high resolution imagery. *Forests*, *7* (7), 138.

Clutter, J.L., Fortson, J.C., Pienaar, L.V., Briester, G.H., & Bailey, R.L. (1983). *Timber managment: A quantitative approach*. John Wiley & Sons, Chichester/New York.

Congalton, R.G., Oderwald, R.G., & Mead, R.A. (1983). Assessing Landsat classification accuracy using discrete multivariate statistical techniques. *Photogrammetric Engineering & Remote Sensing*, *49*, 1671–1678.

Definiens Imaging. 2010. *ECognition developer 8.0.1 reference book*. Retreived March 24, 2014 from: http://www.definiens.com.

Dong, J., Kaufmann, R.K., Myneni, R.B., Tucker, C.J., Kauppi, P.E., Liski, J., … Hughes, M.K. (2003). Remote sensing estimates of boreal and temporate forest woody biomass: Carbon pools, sources, and sinks. *Remote Sensing of Environment*, *84*, 393–410.

Drake, J.B., Dubayah, R.O., Clark, D.B., Knox, R.G., Blair, J.B., Hofton, M.A., … Prince, S.D. (2002a). Estimation of tropical forest structural characteristics using large-footprint Lidar. *Remote Sensing of Environment*, *79*, 305–319.

Drake, J.B., Dubayah, R.O., Knox, R.G., Clark, D.B., & Blair, J.B. (2002b). Sensitivity of large-footprint lidar to canopy structure and biomass in a neotropical rainforest. *Remote Sensing of Environment*, *81*, 378–392.

Envi - Reference Guide. (2009). *Exelis visual information solutions*. Boulder, Colorado: Exelis Visual Information Solutions.

Esri. (2010). *ArcGIS Desktop: Release 10*. Redlands, CA: Environmental Systems Research Institute.

Ferreira, L.G., Ferreira, N.C., & Ferreira, M.E. (2008). *Sensoriamento remoto da vegetação: Evolução e estado-da-arte* [Remote Sensing of vegetation: Evolution and state of the art].Acta Scientiarum. *Biological Sciences*, *30*, 379–390.

Flombaum, P., & Sala, O.E. (2007). A non-destructive and rapid method to estimate biomass and aboveground net primary production in arid environments. *Journal of Arid Environments*, *69*, 352–358.

Foody, G.M., Boyd, D.S., & Cutler, M.E.J. (2003). Predictive relations of tropical forest biomass from Landsat TM data and their transferability between regions. *Remote Sensing of Environment*, *85*, 463–474.

Forey, P. (1996). *Árvores: Guia prático para reconhecer todos os tipos de árvores [Trees: Pratical guide to recognizing all types of trees]*. Lisboa: Pequenos Guias da Natureza.

Foroughbakhch, R., Reyes, G., Alvarado-Vázquez, M.A., Hernández-Piñero, J., & Rocha-Estrada, A. (2005). Use of quantitative methods to determine leaf biomass on 15 woody shrub species in northeastern México. *Forest Ecology and Management*, *216*, 359–366.

Frohn, R.C., Autrey, B.C., Lane, C.R., & Reif, M. (2011). Segmentation and object-oriented classification of wetlands in a karst Florida landscape using multi-season Landsat-7 ETM+ imagery. *International Journal of Remote Sensing*, *32*, 1471–1489.

Ghiyamat, A., Shafri, H.Z.M., & Shariff, A.R.M. (2016). Influence of tree complexity on discrimination performance of vegetation indices. *European Journal of Remote Sensing*, *49*, 15–37.

Gómez, C., Wulder, M.A., Montes, F., & Delgado, J.A. (2012). Modelling forest structural parameters in Mediterranean pines of central Spain using QuickBird-2 Imagery and classification and regression tree analysis (CART). *Remote Sensing*, *4*(1), 135–159.

Günlü, A., Ercanli, I., Sönmez, T., & Baskent, E.Z. (2014). Prediction of some stand parameters using pan-sharpened IKONOS satellite image. *European Journal of Remote Sensing*, *47*, 329–342.

Hall, R.J., Skakun, R.S., Arsenault, E.J., & Case, B.S. (2006). Modeling forest stand structure attributes using Landsat ETM+ data: Application to mapping of aboveground biomass and stand volume. *Forest Ecology and Management*, *225*, 378–390.

Häme, T., Salli, A., Andersson, K., & Lohi, A. (1997). A new methodology for estimation of biomass of conifer-dominated boreal forest using NOAA AVHRR data. *International Journal of Remote Sensing*, *18*, 3211–3243.

Hirata, Y., Tabuchi, R., Patanaponpaiboon, P., Pougparn, S., Yoneda, R., & Fujioka, Y. (2014). Estimation of aboveground biomass in mangrove forest using high-resolution satellite data. *Journal of Forest Research*, *19*, 34–41.

Houghton, R.A. (2005). Aboveground forest biomass and the global carbon balance. *Global Change Biology*, *11*, 945–958.

Huete, A., Liu, H.G., Batchily, K., & Leeuwen, W.J.D.V. (1997). A comparison of vegetation indices over a global set of TM images for EOS-MODIS. *Remote Sensing of Environment*, *59*, 440–451.

Huete, A., Miura, T., Yoshioka, H., Ratana, P., & Broich, M. (2014). Indices of vegetation activity. In J. Hanes (Ed.), *Biophysical applications of satellite remote sensing (pp.1-38)*. Berlin Heidelberg: Springer-Verlag.

Huete, A.R. (1988). A soil-adjusted vegetation index (SAVI). *Remote Sensing of Environment*, *25*, 295–309.

Huete, A.R., Justice, C., & Van Leuwen, W. (1996). *MODIS vegetation index (MOD13), Algorithm theoretical basis document, version 2*. Tucson, USA: University of Arizona.

IFN5. (2010). *Inventário Florestal Nacional* [National forest inventory]. *IFN5 2005-2006. Portugal Continental*. Lisboa, Portugal: Autoridade Florestal Nacional.

Jackson, R.D., & Huete, A.R. (1991). Interpreting vegetation indices. *Preventive Veterinary Medicine*, *11*, 185–200.

Jensen, J.R. (2000). *Remote sensing of the environment: An earth resource perspective*. Upper Saddle River, NJ: Prentice-Hall

Ji, L., Wylie, B.K., Nossov, D.R., Peterson, B., Waldrop, M.P., McFarland, J.W., … Hollingsworth, T.N. (2012). Estimating aboveground biomass in interior Alaska with data and field measurements. *International Journal of Applied Earth Observation and Geoinformation*, *18*, 451–461.

Jordan, C.F. (1969). Derivation of leaf area index from quality of light on the forest floor. *Ecology*, *50*, 663–666.

Lu, D. (2006). The potential and challenge of remote sensing-based biomass estimation. *International Journal of Remote Sensing*, *27*, 1297–1328.

Maack, J., Kattenborn, T., Fassnacht, E., Enble, F., Hernández, J., Corvalán, P., & Koch, B. (2015). Modeling forest biomass using very-high-resolution data - Combining textural, spectral and photogrammetric preditors derived from spaceborne stereo images. *European Journal of Remote Sensing*, *48*, 245–261.

Maciel, M.N.M., Bastos, P.C.O., Carvalho, J.O.P., & Watrin, O.S. (2009). *Uso de imagens orbitais na estimativa de parâmetros estruturais de uma floresta primária no município de Paragominas, Estado do Pará* [Use of orbital images in the estimation of structural parameters of a primary forest in the city of Paragominas, State of Pará]. *Revista Ciência Agrária*, *52*, 159–178.

McRoberts, R., Tomppo, E., & Naesset, E. (2010). Advanced and emerging issues on national forest inventories. *Scandinavian Journal of Forest Research*, *25*, 368–381.

Melo, A.C.G., & Durigan, G. (2006). Fixação de carbono em reflorestamento de matas ciliares no Vale do Paranapanema. *Scientia Forestalis*, *71*, 149–154.

Montgomery, D.C., & Peck, E.A. (1982). *Introduction to linear regression analysis*. John Wiley & Sons, New York.

Mora, B., Wulder, M.A., White, J.C., & Hobart, G. (2013). Modeling stand height, volume, and biomass from very high spatial resolution satellite imagery and samples of airborne LiDAR. *Remote Sensing*, *5*(5), 2308–2326.

Mutanga, O., Adam, E., & Cho, M.A. (2012). High density biomass estimation for wetland vegetation using WorldView-2 imagery and random forest regression algorithm. *International Journal of Applied Earth Observation and Geoinformation*, *18*, 399–406.

Mutanga, O., & Skidmore, A.K. (2004). Narrow band vegetation indices overcome the saturation problem in biomass estimation. *International Journal of Remote Sensing*, *25*, 1–16.

Muukkonen, P., & Heiskanen, J. (2007). Biomass estimation over a large area based on standwise forest inventory data and ASTER and MODIS satellite data: A possibility to verify carbon inventories. *Remote Sensing of Environment*, *107*, 617–624.

Myers, R.H. (1986). *Classical and modern regression with applications*. Boston: Duxbury Press.

Navulur, K. (2006). *Multispectral image analysis using the object-oriented paradigm*. New York, NY: Taylor and Francis.

Nelson, B.W., Mesquita, R., Pereira, J., Souza, S.G., Batista, G., & Couto, L.B. (1999). Allometric regressions for improved estimate off secondary forest biomass in the central Amazon. *Forest Ecology and Management*, *117*, 149–167.

Nguyen, H.C., Jung, J., Lee, J., Choi, S.-U., Hong, S.-U., & Heo, J. (2015). Optimal atmospheric correction for above-ground forest biomass estimation with the ETM + remote sensor. *Sensors*, *15*, 18865–18886.

Palace, M., Keller, M., Asner, G.P., Hagen, S., & Braswell, B. (2008). Amazon forest structure from IKONOS satellite data and the automated characterization of forest canopy properties. *Biotropica*, *40*, 141–150.

Palacios-Orueta, A., Chuvieco, E., Parra, A., & Carmona-Moreno, C. (2005). Biomass burning emissions: A review of models using remote sensing data. *Environmental Monitoring and Assessment*, *104*, 189–209.

Parresol, B.R. (1999). Assessing tree and stand biomass: A review with examples and critical comparisons. *Forest Science*, *45*, 573–593.

Paulo, J.A., & Tomé, M. (2006). *Equações para estimação do volume e biomassa de duas espécies de carvalhos: Quercus suber e Quercus ilex. Publicações do GIMREF; RC1*. Lisboa: Instituto Superior de Agronomia. Departamento de Engenharia Florestal.

Peichl, M., & Arain, M.A. (2006). Above and belowground ecosystem biomass and carbon pools in an age-sequence of temperate pine plantation forests. *Agricultural and Forest Meteorology*, *140*, 51–63.

Pereira, J.M.C., Oliveira, T.M., & Paul, J.C.P. (1995). Satellite-based estimation of Mediterranean shrubland structural parameters. *EARSeL Advances in Remote Sensing*, *4*, 14–20.

Pinheiro, E.S., Durigan, G., & Adami, M. (2009). Imagens Landsat e QuickBird são capazes de gerar estimativas precisas de biomassa aérea de Cerrado? In INPE (Ed.), *XIV Simpósio Brasileiro de Sensoriamento Remoto, Anais XIV Simpósio Brasileiro de Sensoriamento Remoto* (pp. 2913–2920). Brazil: São José dos Campos.

Ponzoni, F.J., & Shimabukuro, Y.E. (2007). *Sensoriamento remoto no estudo da vegetação. Editora Parêntese*. São José dos Campos: Oficina de textos.

Popescu, S.C., Wynne, R.H., & Nelson, R.F. (2003). Measuring individual tree crown diameter with lidar and assessing its influence on estimating forest volume and biomass. *Canadian Journal of Remote Sensing*, *29*, 564–577.

Potter, C. (1999). Terrestrial biomass and the effects of deforestation on the global carbon cycle. *BioScience*, *49*, 769–778.

Pretzsch, H. (2009). *Forest dynamics, growth and yield: From measurement to model*. Berlin: Springer-Verlag.

Rauste, J., & HäMe, T. (1994). Radar-based forest biomass estimation. *International Journal Of Remote Sensing*, *15*, 2797–2808.

Ren, H., & Zhou, G. (2014). Determination of green above-ground biomass in desert steppe using litter-soil adjusted vegetation index. *European Journal of Remote Sensing*, *47*, 611–625.

R Development Core Team, (2012). R: A language and environment for statistical computing. R Foundation for Statistical Computing, http://www.R-project.org. (Accessed 21 February, 2016).

Rizzi, R. (2004). *Geotecnologias em um sistema de estimativa da produção de soja: Estudo de caso no Rio Grande do Sul. Tese de Doutorado*. São José dos Campos: Instituto Nacional de Pesquisas Espaciais.

Rouse, J.W., Haas, R.H., Schell, J.A., & Deering, D.W. 1973. *Monitoring vegetation systems in the great plains with ERTS*. In 3rd ERTS Symposium, NASA SP-351 I. 309–317.

Ryu, S.R., Chen, J., Crow, T.R., & Saunders, S.C. (2004). Available fuel dynamics in nine contrasting forest ecosystems in north America. *Environmental Management*, *33*, 87–107.

Segura, M., & Kanninen, M. (2005). Allometric models for tree volume and total aboveground biomass in a tropical humid forest in Costa Rica. *Biotropica*, *37*, 2–8.

Shapiro, S.S., Wilk, M.B., & Chen, H.J. (1968). A comparative study of various tests of normality. *Journal of the American Statistical Association*, *63*, 1343–1372.

Sheskin, D.J. (2007). *Handbook of parametric and nonparametric statistical procedures*. 4th Edition, Boca Raton, Florida: Chapman & Hall/CRC.

Sousa, A.M.O., Gonçalves, A.C., Mesquita, P., & Marques da Silva, J.R. (2015). Biomass estimation with high resolution satellite images: A case study of Quercus rotundifolia. *ISPRS Journal of Photogrametric and Remote Sensing*, *101*, 69–79.

Sousa, A.M.O., Mesquita, P., Gonçalves, A.C., & Marques da Silva, J.R. (2010). Segmentação e classificação de tipologias florestais a partir de imagens Quickbird. *Ambiência*, *6*, 57–66.

Stehman, S.V. (1996). Estimating the kappa coefficient and its variance under stratified random sampling. *Photogrammetric Engineering & Remote Sensing*, *62*, 401–407.

Steininger, M.K. (2000). Satellite estimation of tropical secondary forest aboveground biomass: Data from Brazil and Bolivia. *International Journal of Remote Sensing*, *21*, 1139–1157.

Thenkabail, P.S., Enclona, E.A., Ashton, M.S., Legg, C., Jean, M., & Dieu, D. (2004). Hyperion, IKONOS, ALI, and ETM+ sensors in the study of African rainforests. *Remote Sensing of Environment*, *90*, 23–43.

Tomppo, E., Nilsson, M., Rosengren, M., Aalto, P., & Kennedy, P. (2002). Simultaneous use of Landsat-TM and IRS-1c WiFS data in estimating large area tree stem volume and aboveground biomass. *Remote Sensing of Environment*, *82*, 156–171.

Valdés, B., Talavera, S., & Fernández-Galiano, E. (1987). Flora Vascular de. *Andalucía Occidental*, *1*(2), 3.

Van Der Meer, F., Bakker, W., Scholte, K., Skidmore, A., De Jong, S., Cleves, J., … Epema, G. (2016). Spatial scale variations in vegetation indices and above-ground biomass estimates: Implications for Meris. *International Journal of Remote Sensing*, *22*, 3381–3396.

Vaz, M., Maroco, J., Ribeiro, N., Gazarini, L.C., Pereira, J. S., & Chaves, M.M. (2011). Leaf-level responses to light in two co-occurring Quercus (Quercus ilex and Quercus suber): Leaf structure, chemical composition and photosynthesis. *Agroforestry Systems*, *82*, 173–181.

Viana, H., Aranha, J., Lopes, D., & Cohen, W.B. (2012). Estimation of crown biomass of Pinus pinaster stands

and shrubland above-ground biomass using forest inventory data, remotely sensed imagery and spatial prediction models. *Ecological Modelling*, *226*, 22–35.

Wang, Q., Adiku, S., Tenhunen, J., & Granier, A. (2005). On the relationship of NDVI with leaf area index in a deciduous forest site. *Remote Sensing of Environment*, *94*, 244–255.

Watzlawick, L.F., & Kirchner, F.F. (2004). Estimativa de biomassa e carbono utilizando imagens de satélite de alta resolução. In C.R. Sanquetta, R. Balbinot, & M.A.A. Ziliotto (Eds.), *Fixação de carbono: Atualidades, projetos e pesquisas. Curitiba, Brasil* (pp. 133–152).

Watzlawick, L.F., Kirchner, F.F., & Sanquetta, C.R. (2009). Estimativa de biomassa e carbono em floresta com araucária utilizando imagens do satélite Ikonos II. *Ciência Florestal*, *19*, 169–181.

Watzlawick, L.F., Koehler, H.S., & Kirchner, F.F. (2006). Estimativa de biomassa e carbono em plantios de Pinus taeda L. utilizando imagens do satélite IKONOS II. *Ciência e Natura*, *28*, 45–60.

Wulder, M.A., Hall, R.J.N.C., & Franklin, S.E. (2004). High spatial resolution remotely sensed data for ecosystem characterization. *BioScience*, *54*, 511–521.

Yin, G., Zhang, Y., Sun, Y., Wang, T., Zeng, Z., & Piao, S. (2015). MODIS based estimation of forest above-ground biomass in China. *PLoS ONE*, *10*(6), e0130143.

Zanzarini, F.V., Pissara, T.C.T., Brandão, F.J.C., & Teixeira, D.D.B. (2013). Correlação espacial do índice de vegetação (NDVI) de imagem Landsat/ETM+ com atributos do solo. *Revista Brasileira de Engenharia Agrícola e Ambiental*, *17*, 414–608.